Modal analysis reveals imprint of snowflake shape on wake flow structures

Giorgia Tagliavini, Markus Holzner, Pascal Corso

Supplementary material

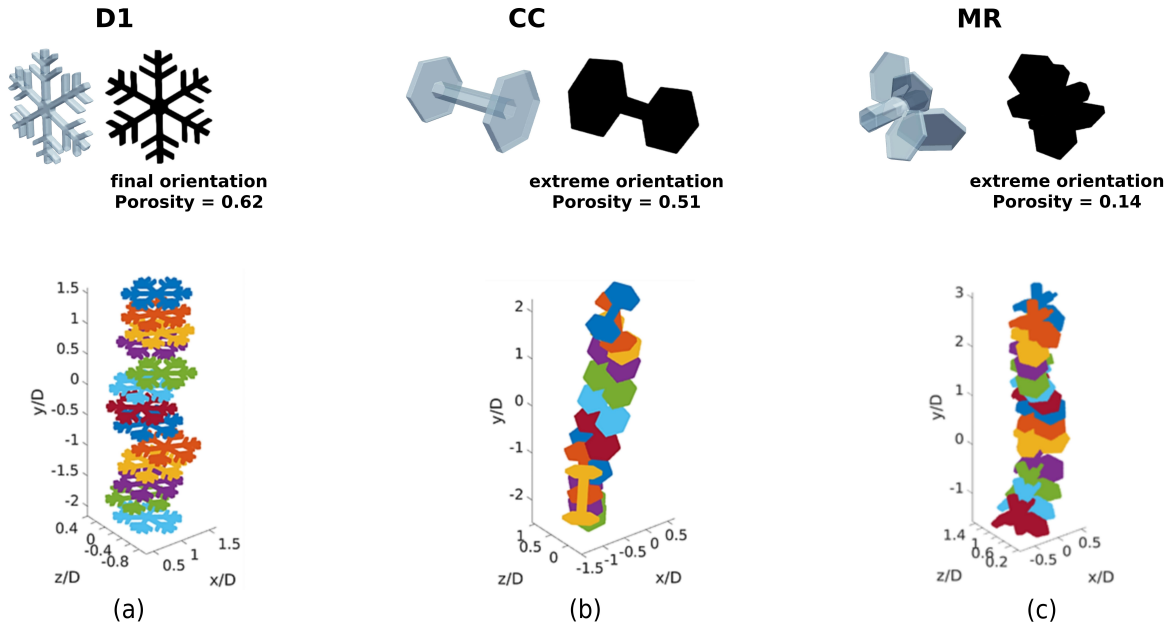

Figure A1: 3D geometries (blue) and projected areas (black) of the investigated snow particles, as examples of common classes of snow particles observed in nature (Kikuchi et al., 2013). The projected area shown in the figure for each particle is the one used in the computational model (orthogonal to the flow direction). It corresponds to the final orientation for **D1** (a) and most frequently occurring among the extreme orientations observed during the free-fall of **CC** (b) and **MR** (c). The figure also reports the instantaneous positions reconstructed from the experiments to stress the difference between the steady falling behavior of **D1** (a) and the unsteady motion of **CC** (b) and **MR** (c). The names of the geometries are abbreviations of the nomenclature used by McCorquodale and Westbrook (2020b).

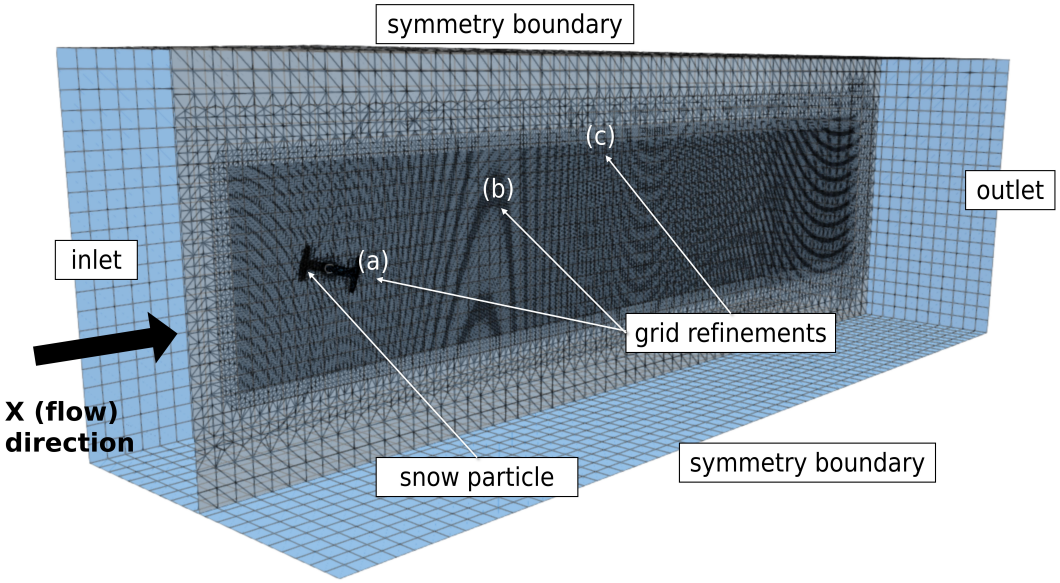

Figure A2: 3D computational domain and grid. The boundaries and the grid refinements are indicated. In particular, three mesh refinement regions are specified. The base grid is built using *blockMesh* (OpenFOAM, 2017).

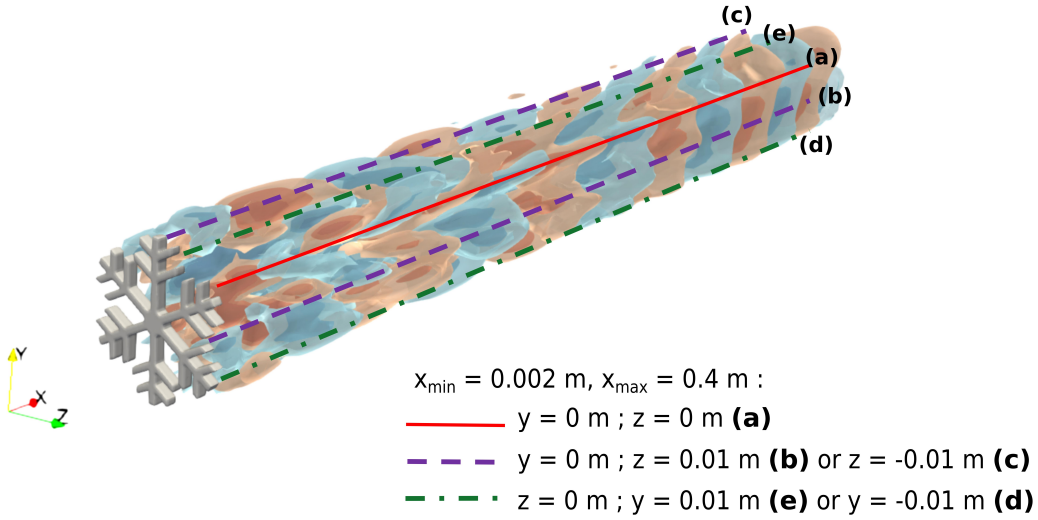

Figure A3: Visual representation of the sampling lines used to investigate the spatial distribution of POD and DMD modes. For each line, 2000 sampling points are employed (see Section 4.4).

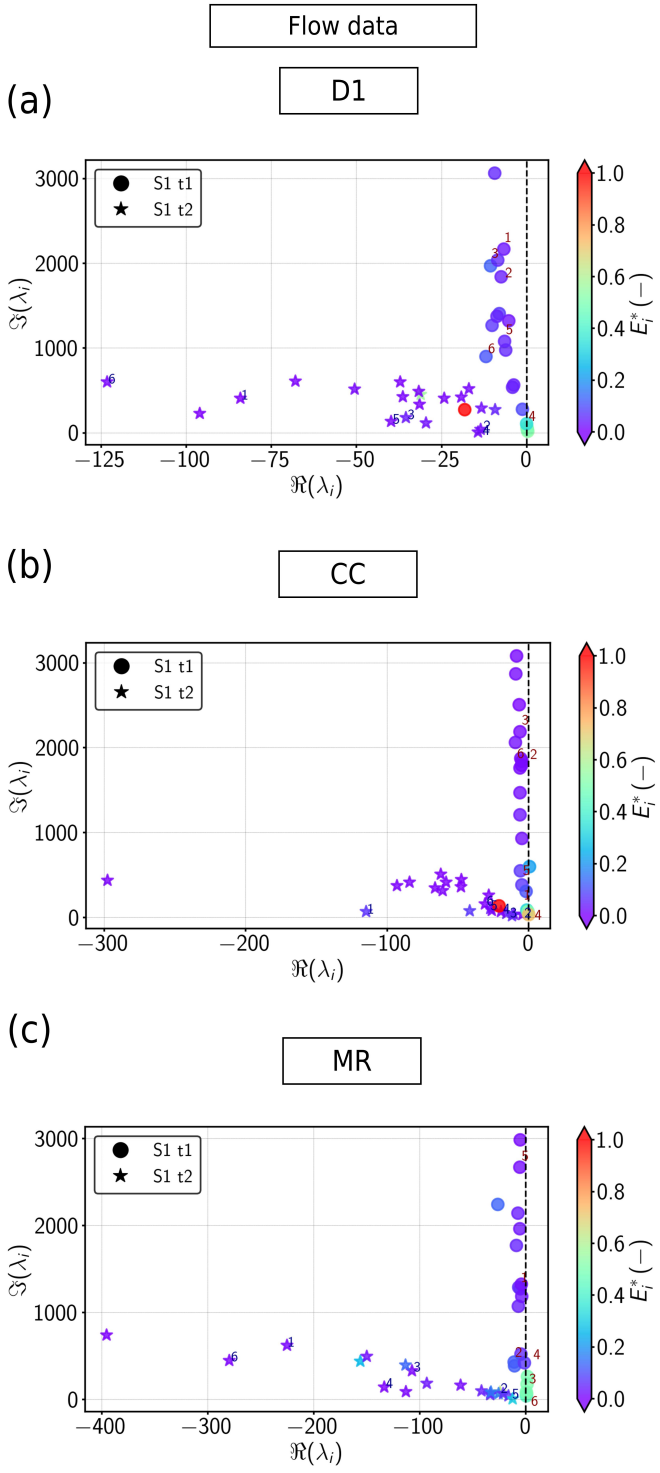

Figure A4: Complex plane showing the distribution of the first 20 DMD exponential eigenvalues λ_i^{DMD} for all the three snowflake geometries at both sampling rates (Δt_1 and Δt_2) for data set ***S1***.

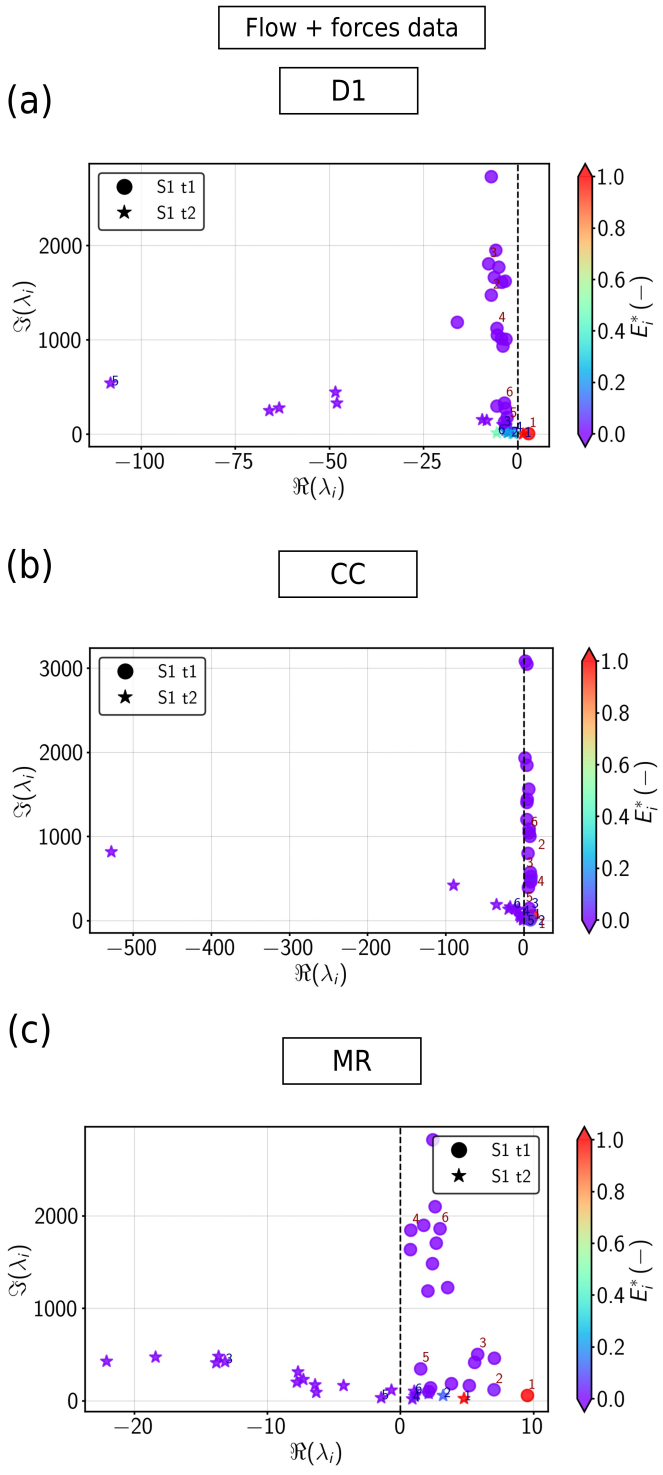

Figure A5: Complex plane showing the distribution of the first 20 DMD exponential eigenvalues λ_i^{DMD} for all the three snowflake geometries at both sampling rates (Δt_1 and Δt_2) for data set ***S3***.

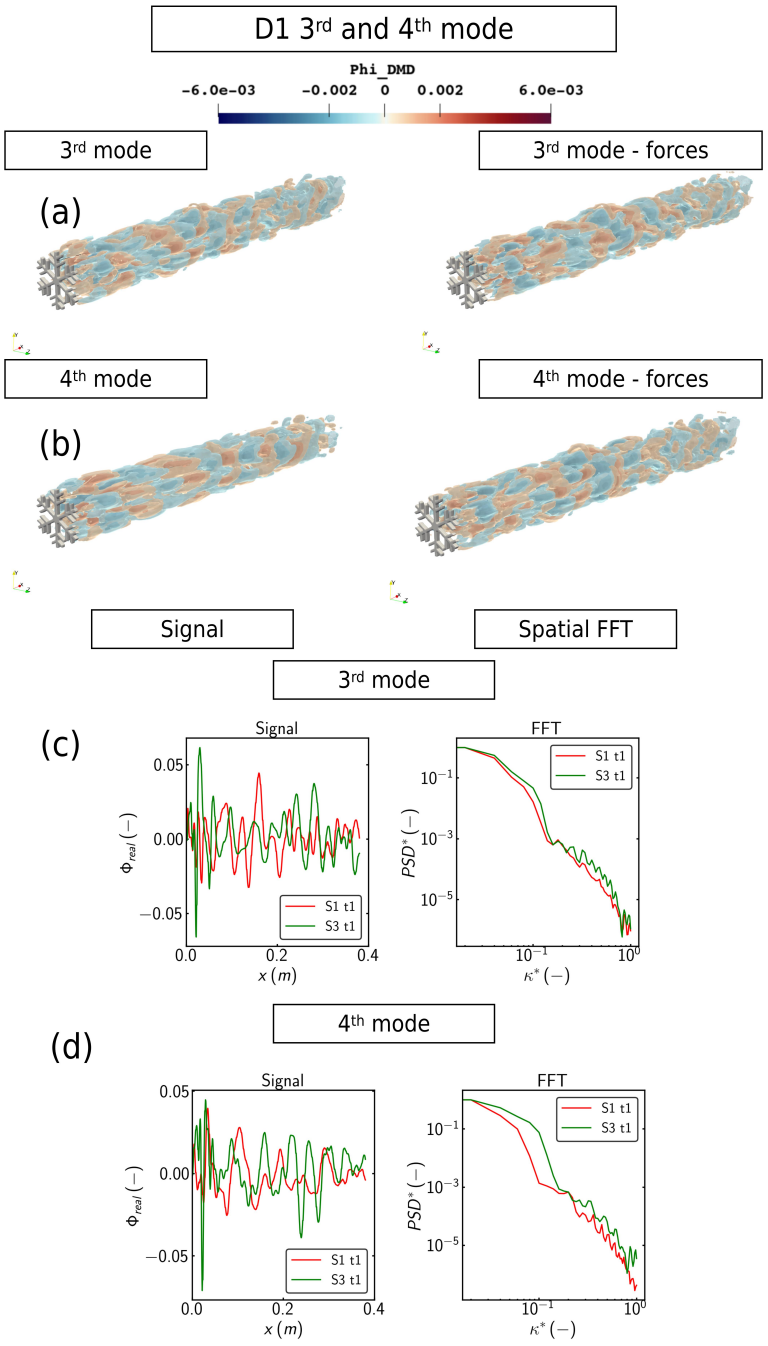

Figure A6: Third and fourth mode resulting from Dynamic Mode Decomposition performed on the numerical data (left) and the numerical data with the forces included in the snapshot matrix (right), pertaining to particle **D1**. The top part of the figure qualitatively illustrates the spatial distribution of the third (a) and the fourth (b) mode, while the bottom part shows the quantitative comparison between the spatial signals and their power spectral density of ***S1*** and ***S3*** for the third (c) and fourth (b) DMD mode. The power spectral density and wavenumber are normalized with their maximum values (see Section 2.4).

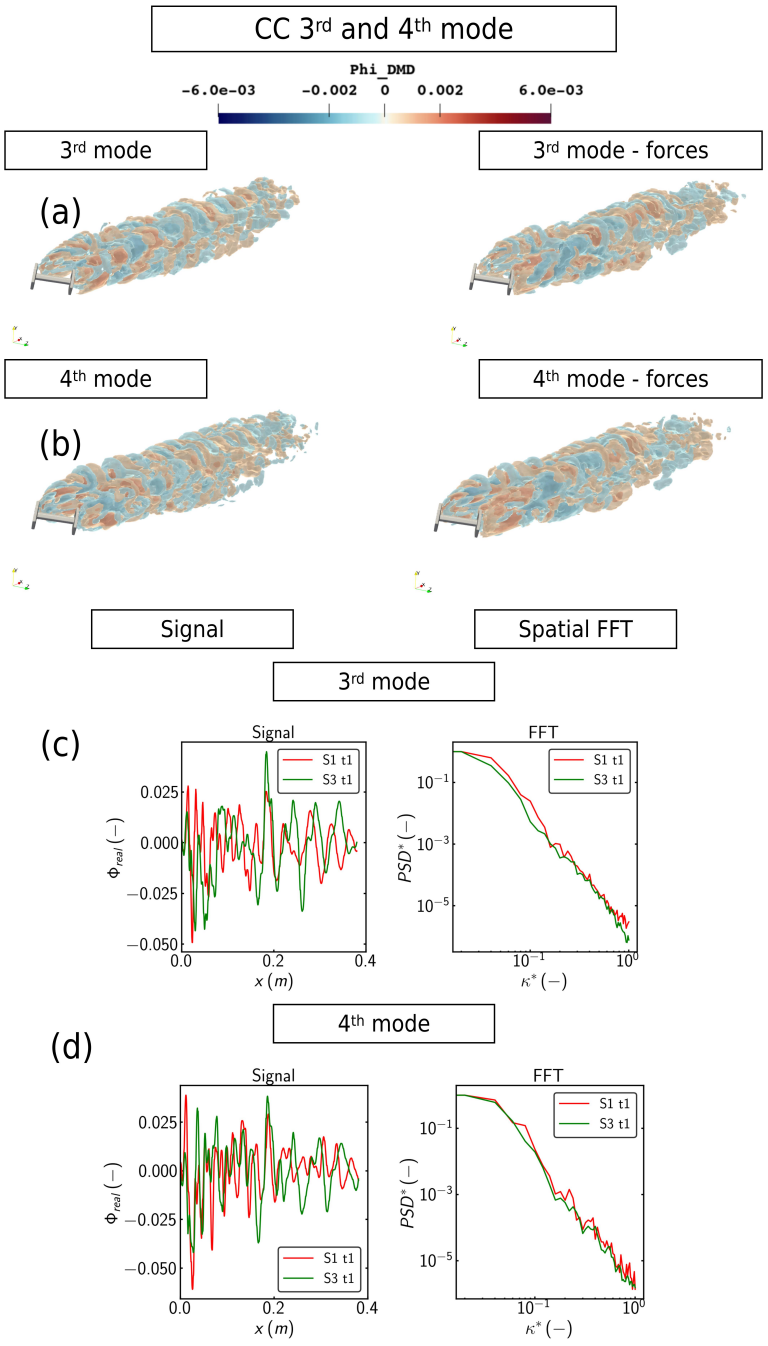

Figure A7: Third and fourth mode resulting from Dynamic Mode Decomposition performed on the numerical data (left) and the numerical data with the forces included in the snapshot matrix (right), pertaining to particle **CC**. The top part of the figure qualitatively illustrates the spatial distribution of the third (a) and the fourth (b) mode, while the bottom part shows the quantitative comparison between the spatial signals and their power spectral density of ***S1*** and ***S3*** for the third (c) and fourth (b) DMD mode. The power spectral density and wavenumber are normalized with their maximum values (see Section 4.4).

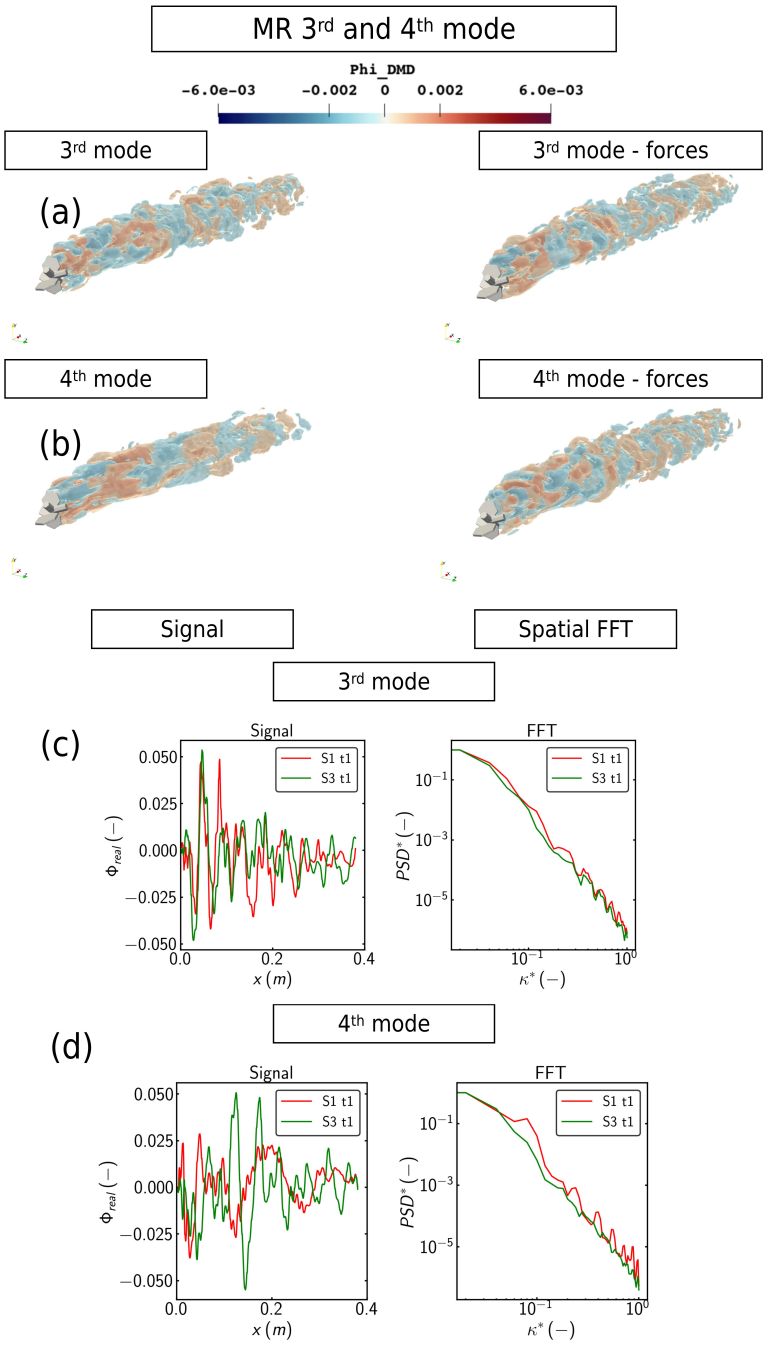

Figure A8: Third and fourth mode resulting from Dynamic Mode Decomposition performed on the numerical data (left) and the numerical data with the forces included in the snapshot matrix (right), pertaining to particle **MR**. The top part of the figure qualitatively illustrates the spatial distribution of the third (a) and the fourth (b) mode, while the bottom part shows the quantitative comparison between the spatial signals and their power spectral density of ***S1*** and ***S3*** for the third (c) and fourth (b) DMD mode. The power spectral density and wavenumber are normalized with their maximum values (see Section 4.4).

Table A1: Values of the slope s of the linear fitting from Figure 12 and 13 for the original data set ***S1*** and the one with the inclusion of the forces ***S3***. The slope is evaluated as $s = \beta/\epsilon$, with ϵ being the particle shape porosity and β being one of the compared quantities from DMD, i.e. $\Re(\lambda_i)_{min}$, $\Re(\lambda_i)_{max}$, γ_{min}, γ_{max}, $\kappa^{d,*}_{min}$, or $\kappa^{d,*}_{max}$.

Slope (s)	$\Re(\lambda_i)_{min}$	$\Re(\lambda_i)_{max}$	γ_{min}	γ_{max}	$\kappa^{d,*}_{min}$	$\kappa^{d,*}_{max}$
S1	-7.558	-3.086	-0.898	-23.860	0.405	17.935
S3	-19.553	-13.257	-3.984	-11.667	0.425	15.485